Flow of ice through converging channels

Kubat, Ivana; Sayed, Mohamed; Savage, S.; Carrieres, T.

Publisher's version / Version de l'éditeur:

Proceedings of the Sixteenth (2006) International Offshore and Polar Engineering Conference, 1, pp. 577-583, 2006-05

Proceedings of the Sixteenth (2006) International Offshore and Polar Engineering Conference
San Francisco, California, USA, May 28-June 2, 2006

ISBN 1-880653-66-4 (Set); ISSN 1098-6189 (Set)

Flow of ice through converging channels

I.Kubat[1], M.Sayed[1], S.B.Savage[2] and T.Carrieres[3]
[1]Canadian Hydraulics Centre, National Research Council of Canada
Ottawa, ON, Canada
[2] McGill University
Montreal, PQ, Canada
[3] Canadian Ice Service, Environment Canada
Ottawa, ON, Canada

ABSTRACT

This paper presents predictions of the flow of ice in wedge-shaped converging channels. Such flows are encountered in the relatively constricted waters of the Canadian Arctic Archipelago. Ridging, lead opening patterns, development of high-pressure area, and arch formation are some of the processes present during ice flow through converging channels. An idealized geometry was used in the testing to represent many of the areas typical in the Canadian Arctic Archipelago. The results show the ice cover flow, distribution of stresses, ice thickness, area coverage, ridging, and arch formation at the constricted exit of the channel. The effects of thermodynamic growth and melt are neglected as the forecasts cover durations of only few days.

KEY WORDS: converging channel; ice flow; ice thickness; ice concentration; level ice; ridged ice; ice advection; forecast.

INTRODUCTION

The flow of ice in constricted channels displays several unique characteristics. Land boundaries of such channels can influence velocity distributions, ridging patterns and the formation of ice arches. Those conditions are encountered in regions such as the Canadian Arctic Archipelago. The present study considers ice flow in a converging channel, which may be representative of many regions in the Archipelago. The focus is on short-term behaviour. Therefore, only mechanical deformation of the ice cover is considered in the analysis.

Sodhi (1977) considered the analogy between the flow of ice in converging channels and that of granular materials in hoppers. He used Jenike's (1964) early analysis of arching, which assumes that deformation is governed by a cohesive Mohr-Coulomb criterion. Sodhi (1977) then examined LANDSAT imagery for Amundsen Gulf and the Bering Strait to estimate the values of cohesion which would produce arches. Erlingsson (1991) later examined the deformation of ice near shorelines by analyzing satellite imagery. He was able to determine the directions of the characteristics for the deformation field. Using a Mohr-Coulomb yield criterion, the directions of the characteristics were used to infer values for the angle of internal friction.

Simulations of the flow of ice in converging channels were done by Gutfraind and Savage (1998). They employed two numerical methods: Smooth-Particle-Hydrodynamics (SPH) and a discrete element approach. The SPH simulations were based on a cohesionless Mohr-Coulomb criterion. The resulting velocity and stress distributions showed agreement between the two approaches. More recent related studies mostly utilized remote sensing observations. For example, Kwok and Rothrock (1999) examined the flow of ice in the Fram Strait. Ice flux through Nares Strait has been the subject of recent studies by Samelson et al. (2005) and by Kwok (2005).

In the present study, the dynamics of ice flow in wedge-shaped channels is examined. Calculations are done using a dynamics model that solves the continuity, momentum and plastic yield equations. A thickness redistribution model is also used to account for ridge building. The distributions of stresses and velocities are determined, and the role of various parameters is examined. In particular, the conditions leading to the formation of an ice arch are examined.

THE MODEL

The dynamics model has been described in a number of past publications (e.g. Sayed and Carrieres, 1998; and Sayed et al., 2002). The thickness redistribution formulation has also been examined by Kubat et al. (2005). Therefore, only a brief overview of the model is given here. The dynamics model solves the equations of balance of mass and momentum. The momentum equation considers the forces acting on the ice cover due to air and water drag, Coriolis force, and water surface tilt. In addition, constitutive equations are needed to relate the stresses and strain rates. Hibler's (1979) plastic yield envelope, which has the form of an ellipse in the principal stress space as shown in Fig. 1, is used. The ratio between the major and minor principal axes of the ellipse (usually expressed by the symbol "*e*"), can be viewed as a measure of the *shear strength* of the ice cover. A large value of e represents an elongated ellipse, with relatively small shear strength. Conversely, a small value of e represents an ice cover of relatively large shear strength. Hibler's formula (1979), which expresses the normal stress P in terms of ice thickness and area fraction

(concentration), was employed. The equations mentioned in the preceding discussion are not listed here since they are commonly used in ice forecasting literature.

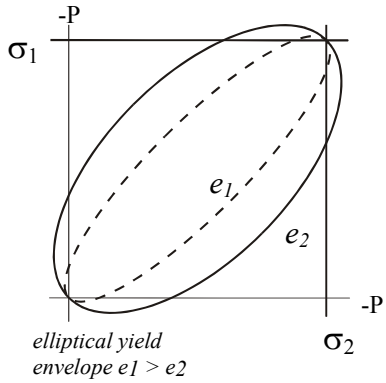

Fig. 1 Schematic of Hibler's (1979) plastic yield envelope.

Thickness Redistribution Model

A thickness redistribution model is needed for closure of the governing equations. The model of Savage (2002) provides a parameterization for the dependence of ridging and lead opening processes on deformation. Kubat et al. (2004) presented discussions and tests of that model. The equations of the thickness redistribution model are briefly listed here.

The area fraction, A and mean thickness, h of the ice cover can be expressed as

$$A = A_c + A_r \tag{1}$$

$$A h = A_c h_c + A_r h_r \tag{2}$$

where the subscripts c and r refer to level (or coherent) ice and ridged (or deformed) ice, respectively. Evolution equations for the thickness and area fraction are derived by considering the continuity and energy balance equations. Those equations depend on the velocity divergence, η, and a redistribution function, ψ. The divergence is given by

$$\eta = \dot{e}_1 + \dot{e}_2 \tag{3}$$

where $\dot{e}_1$ and $\dot{e}_2$, are the principal strain rates. The redistribution function is

$$\psi = \frac{1}{2} A \exp\left[-C\left(1-A\right)\right]\left[\left(\dot{e}_1 + \dot{e}_2\right) - \left[\left(\dot{e}_1 + \dot{e}_2\right)^2 + \frac{\left(\dot{e}_1 - \dot{e}_2\right)^2}{e^2}\right]^{1/2}\right] \tag{4}$$

where the constant C is used in the common expression for ice pressure.

The resulting evolution equations are summarized as follows. The rate of change of the area fraction of ridged and level ice (A_r and A_c, respectively), total area fraction A, ridged ice thickness h_r, and mean ice thickness h, are:

$$\frac{D A_r}{D t} + A_r \eta = \left(1-\beta\right)\psi \tag{5}$$

$$\frac{D A_c}{D t} + A_c \eta = \beta \psi \tag{6}$$

$$\frac{D A}{D t} + A \eta = \psi \tag{7}$$

$$\frac{D h_r}{D t} = \frac{h_r}{A_r}\psi\left[\beta\left(1-\frac{h_c}{h_r}\right)-1\right] \tag{8}$$

$$\frac{D h}{D t} = -\frac{h\psi}{A} \tag{9}$$

The parameter β was derived by considering that the ratio of level ice thickness to ridged ice thickness, h_c/h_r, reaches an asymptotic value (see for example Hopkins, 1998). The resulting expression is

$$\beta = \frac{16.7}{16.7 - h_c^{1/2}} \tag{10}$$

Savage (2002), and Kubat et al. (2004) cover the derivations of the above equations and testing of the model in much more detail.

Numerical Approach

Solution of the momentum equations is done using the semi-implicit method of Zhang and Hibler (1997). The method is based on arranging the terms in the momentum equations, and treating some of them implicitly, while others are treated explicitly. A correction is then introduced to treat the latter terms. An iteration is also used to ensure that the yield condition is satisfied. Details of the present implementation were given by Sayed et al. (2002).

The present approach employs a Particle-In-Cell (PIC) method, where the ice cover is represented by an ensemble of particles. Each particle may be given attributes such as ice thickness, position, and velocity. The particles are advected in a Lagrangian manner. The continuity and momentum equations, however, are solved on a fixed Eulerian grid. That requires mapping of various variables between the particles and the grid.

The original PIC method of Harlow (1964) was used to model fluid flow, and proved to be well suited to handle discontinuities and track moving material boundaries. Subsequent developments by Brackbill et al. (1988) introduced the FLIP method, which reduced numerical dissipation. Sulsky and Brackbill (1991), and Sulsky et al. (1994) extended the method to treat solids, including elastic behaviour, plastic yield, and time-dependent material properties.

In the present implementation, each particle is given the following attributes: thickness and concentration of both level and deformed ice, position, velocity and acceleration. At each time step, the particles are moved to their new positions. Particle attributes are then mapped to a computational grid. The mapping is carried out using bi-linear interpolation functions (see for example Sulsky et al., 1994). The continuity and momentum equations are then solved over the grid. The resulting accelerations and solids volume fractions are mapped back to the particles.

FLOW IN A CONVERGING CHANNEL

The flow of ice in a converging channel is examined in this section. This case is intended to represent situations of flow of ice in constricted channels, typical of areas such the Canadian Arctic Archipelago. Since the forecasts cover durations of only few days, the effects of thermodynamic growth and melt are neglected. The land boundaries form a wedge-shaped channel as shown in Fig. 2.

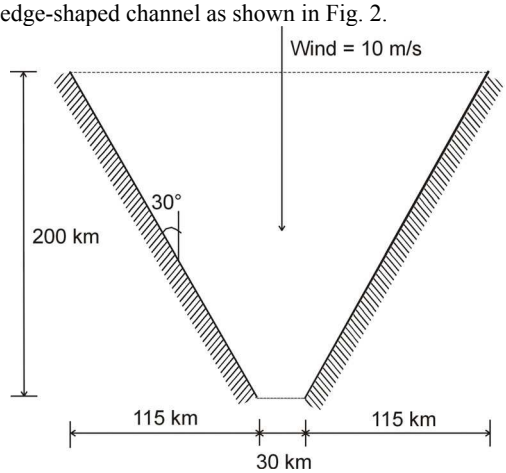

Fig. 2 Test Case Geometry (land boundaries)

The results for a reference case are presented first in detail, then the role of various variables is examined. The ice cover is forced by steady uniform wind of 10 m/s from the North direction. Water current is assumed to be zero in the tests. For the reference case, the ice cover has an initial uniform thickness of 1.0 m, and area coverage of 0.7. The width of the channel at its narrowest point (southern end) is 30 km, and each land boundary lies at a 30° angle to the North (axis of symmetry). The values of other run parameters are:

Time step	5 minutes
Grid cell size	5 km
Air drag coefficient	0.002
Water drag coefficient	0.005
Ice rheological properties(for Hibler's yield envelope):	
Ice strength, p*	10^4 Pa
Elliptical yield envelope axes ratio, e	2
Constant C	20

Coriolis force is set to zero. Therefore, the flow would be symmetrical. The duration of the test is 10 days. Fig. 3 shows snapshots of particle positions (PIC particles used to model advection) after 4 days and 10 days. Those snapshots indicate that the ice move mostly in a *funnel* near the centre of the channel, with relatively little movements near land boundaries. A plot of velocity vectors after 4 days also shows that ice velocities are relatively large within the central *funnel* and that the ice near to the land boundaries is not moving (Fig. 4).

Contours of the mean normal stress (pressure) after 4 days are plotted in Fig. 5. The stresses are lowest near the centerline of the channel, and largest near the land boundaries. The results also show that the free edges at the North and South edges are stress free. The stresses along each boundary increase from the upstream North edge to reach a maximum near the middle, then decreases towards the down stream edge. Gutfraind and Savage (1998) found similar patterns for stress distributions. The present results show that the stresses at the relatively narrow downstream exit form an arch connecting the two land boundaries. Stresses drop sharply as the ice exits the channel.

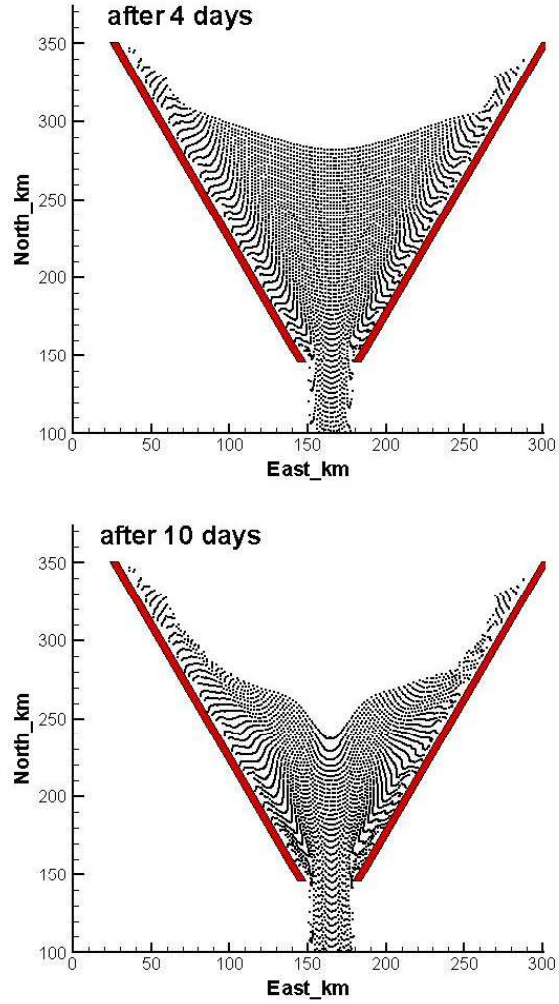

Fig. 3 Snapshots of particle positions after 4 and 10 days

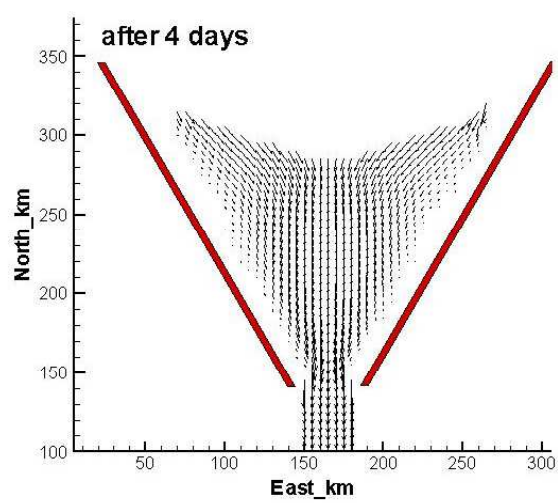

Fig. 4 Ice Velocity after 4 days

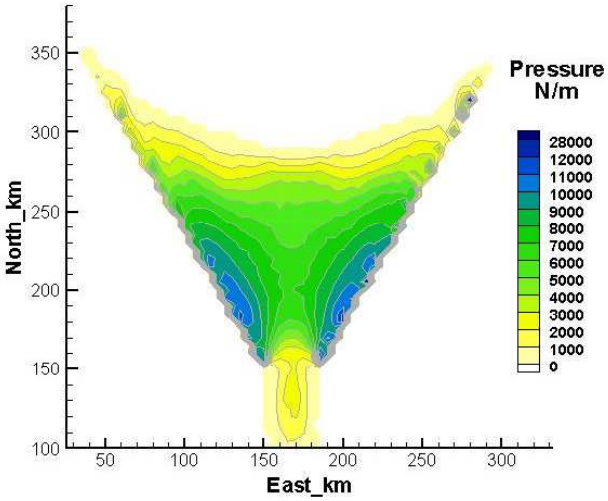

Fig. 5 Mean Normal Stress (pressure) after 4 days

Contour plots of the mean ice thickness h, ridged ice thickness, and area coverage of ridged ice are shown in Fig. 6. As may be expected, ridging occurs in areas of high stresses. The maximum ridged ice thickness is approximately 15 m. The corresponding area coverage of the ridges reaches only 5%. It is noted, however, that the test starts with no ridges at all.

A number of tests were done to examine the role of various variables on ice flow. The forcing wind was found to have relatively significant effect. Fig. 7 shows plots of the velocity near the exit versus time for three values of wind velocity of 10 m/s, 15 m/s, and 20 m/s. Ice velocity was taken as the average of three nodes around the centre line just above the exit, which would give a good measure of ice flux. As may be expected, higher wind velocities produce higher ice velocities. With the ice cover starting from rest, ice velocity increases to reach a near steady state. Since no ice is added at the upstream edge, the nearly steady state velocity is maintained for a limited period until the channel is nearly empty.

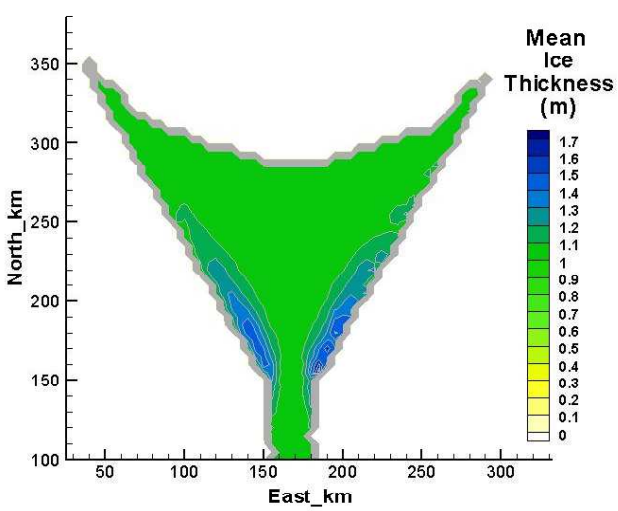

Fig. 6a Mean Ice Thickness after 4 days

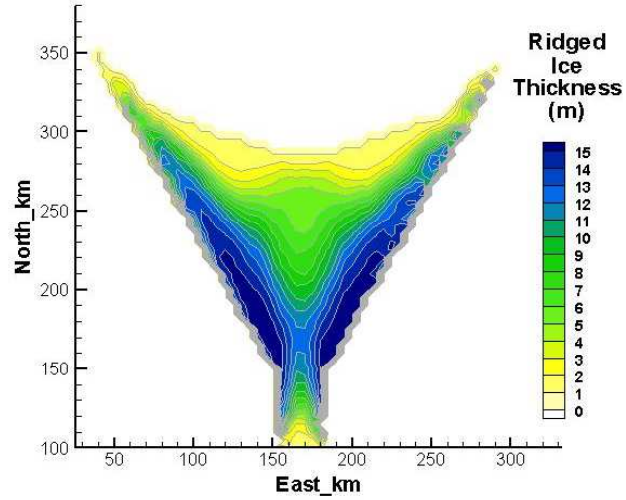

Fig. 6b Ridged Ice Thickness after 4 days

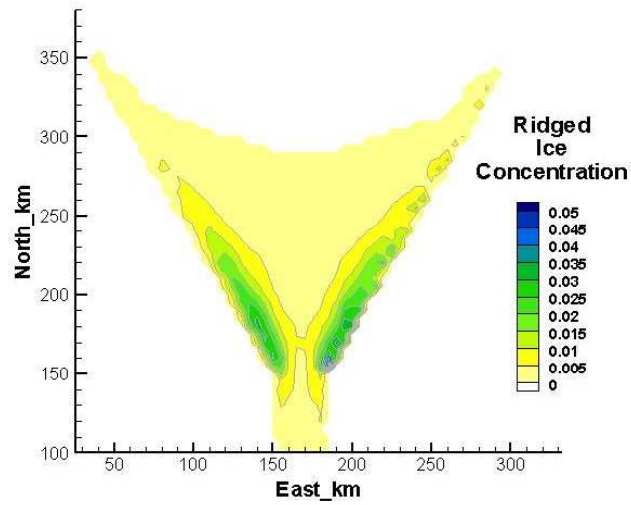

Fig. 6c Ridged Ice Concentration after 4 days

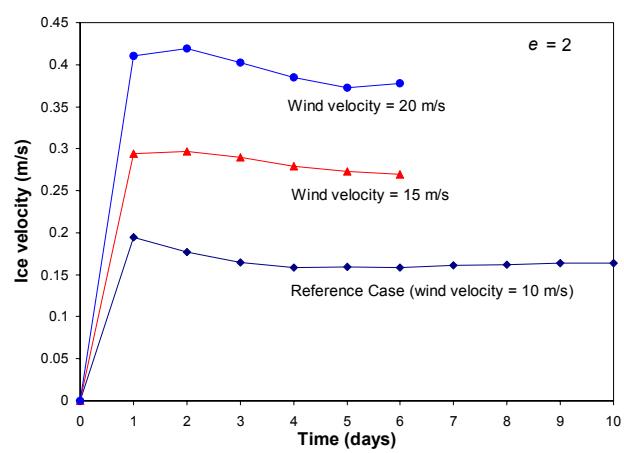

Fig. 7 Average Ice velocity for different wind forcing; measured as the average of three nodes around the centre line just above the exit of the converging channel

Test runs were done using values of initial area coverage of 0.8, 0.9 and 0.95. The resulting flow velocities were similar to those for initial area coverage of 0.7. Tests also showed that the initial ice thickness (values of 0.5 m, 1.0 m, and 2.0 m were used) had little effect on the resulting ice velocities.

Arch Formation

The apparent arch formation at the exit of the channel may govern ice flux and potential blockage. In order to examine the possibility of complete flow blockage, tests were done using different values of ice shear strength. This is achieved by choosing different values of the ratio of the principal axes of the yield ellipse, *e* (Fig. 1). A large value of *e* corresponds to a narrower ellipse and smaller shear strength. Values of *e* = 1.2, 1.5 and 2, were tested. An additional test also examined the case of a so-called *cavitating fluid*, which corresponds to negligible shear strength. The negligible shear was introduced by using a relatively large value of 10 for *e*.

Ice velocities at the exit are plotted versus time in Fig. 8, for the above reference case (with e=2) and a case of higher shear strength (e=1.2). While the velocity is steady for the reference case, using e=1.2 causes the velocity to decelerate after reaching a maximum after one day. That deceleration is apparently coincident with compaction, and pressure build-up, of the ice cover. The flow reaches a complete stop after 5 days, and an arch forms at the exit. Fig. 9 shows contours of the mean normal pressure after the formation of the arch.

For smaller shear strengths (values of e > 1.2) flow continued without arch formation. Fig. 10 shows snapshots of particle positions after 10 days. Those particle positions show the arch at the exit for the case of e=1.2. The positions for the other cases (e > 1.2) illustrate the manner in which shear strength influences ice flow and deformation patterns. It should be emphasized, however, that several other test runs showed that an increase of wind velocity beyond 10 m/s would prevent ice formation for the present ice properties (shear strength corresponding to e=1.2). As may be expected the formation of an arch is a balance between the width of the exit of the channel, ice shear strength, and the driving wind velocity. The results indicate that once ice strength is established (e.g. through validation against field observations), the model can predict the formation of an arch for a particular geometry and forcing conditions.

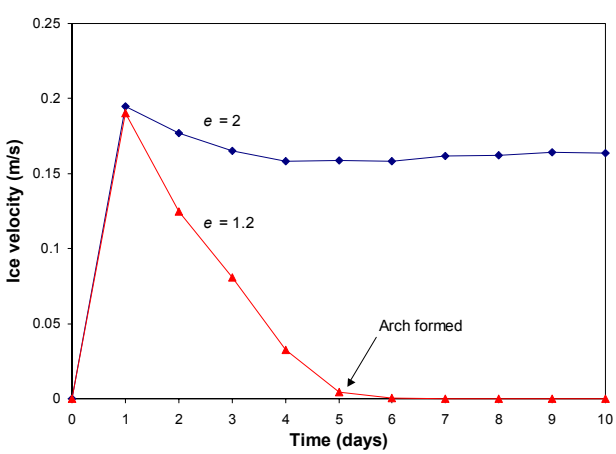

Fig. 8 Ice velocities at the exit of the converging channel for the reference case (with e = 2) and a case of higher shear strength (e = 1.2)

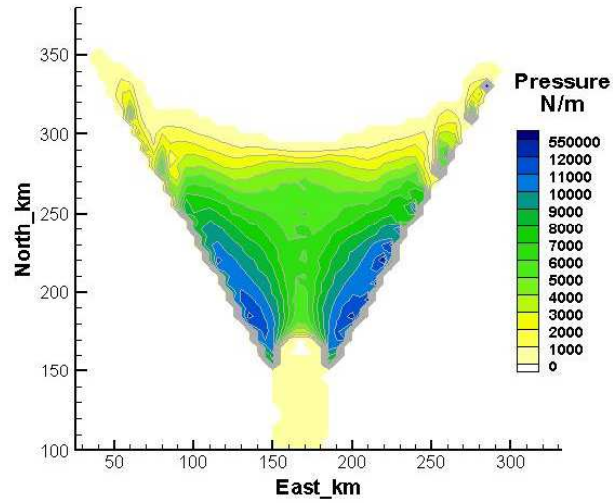

Fig. 9 Mean Normal Stress (pressure) after 5 days for the case of higher shear strength (e = 1.2). Note the arch that stops flow through the opening.

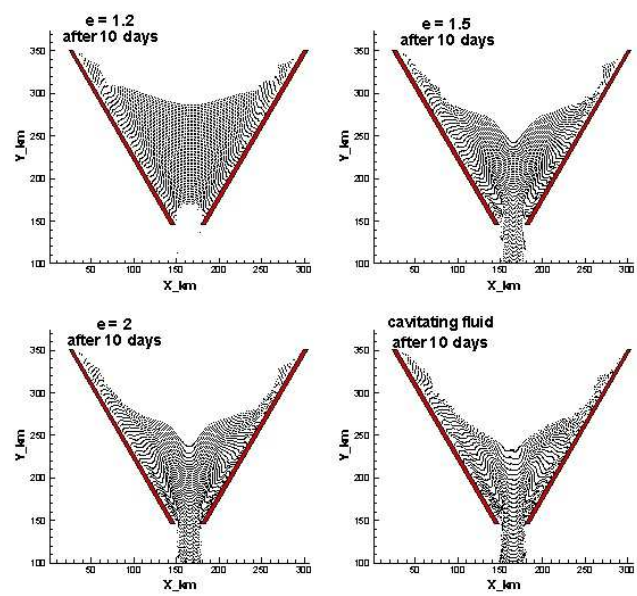

Fig. 10 Snapshots of particle positions after 10 days for cases with different shear strength

Gutfraind and Savage (1998) gave the only available examination of ice flow in converging channels. They used two different numerical methods: Molecular Dynamics and Smooth-Particle-Hydrodynamics (SPH). The Molecular Dynamics calculations are based on tracking the movements of individual disc-shaped particles, and evaluating contact forces between them. The SPH model solves the continuum governing equations over an assembly of particles, which agrees with the general approach of the present PIC method. There are some differences, however, between the SPH governing equations of Gutfraind and Savage (1998) and the present model. Their calculations used a Mohr-Coulomb plastic yield condition instead of the present elliptical yield envelope. Water and drag coefficients had linear dependence on velocities (the present drag formulas are quadratic). Perhaps the major difference is, unlike the present model, they did not introduce ridging (or thickness redistribution).

Direct quantitative comparison between the present results and those of Gutfraind and Savage is difficult because of the issues mentioned above. However, both studies produced flow patterns that agree qualitatively. For example, stress distributions are similar. They show stresses higher at the land boundaries than at the centre of the channel. They also show that stresses along each land boundary increase from the upstream boundary to reach a maximum near mid-distance, then decrease towards the downstream end. Ice velocity distributions across the width of the channel are also similar, with maximum ice velocities occurring near the centre, and decreasing towards the land boundaries.

A test run was conducted in an attempt to obtain more quantitative comparisons with the results of Gutfraind and Savage (1998). The parameters were kept the same as listed for the reference case mentioned earlier in this paper. The exception was to use a 70 km wide exit for the converging channel. The present model gave maximum ice velocities of approximately 0.2 m/s, along an East-West section mid-way between the upstream and downstream ends of the channel. The corresponding velocities obtained by Gutfraind and Savage (their Fig. 11) were between 0.075 and 0.1 m/s. Aside from the several differences between the models (discussed above), the higher velocities of the present model may be due to the introduction of thickness redistribution (or ridging). In the case of Gutfraind and Savage (1998), the ice was not allowed to undergo *out-of-plane* deformation or thickening, which in turn would incur more resistance to flow through the channel.

CONCLUSIONS

The present study examined the flow of ice in wedge-shaped converging channel. An idealized geometry was used to represent many of the areas typical in the Canadian Arctic Archipelago. Deformation of the ice cover due to mechanical deformation was considered without including thermodynamic growth and melt, which corresponds to relatively short durations. The dynamics model used in the present work employs Hibler's (1979) elliptical yield envelope, a Zhang-Hibler numerical solution, and Particle-In-Cell (PIC) advection scheme. The thickness redistribution model of Savage (2002) was used to account for possible ridging and lead opening.

The results show that the ice cover flows predominantly in a *funnel* at the centre of the channel. Velocities (and displacements) are relatively small near the land boundaries. It is possible that ice in such zones of small deformation may be amenable to thermal consolidation and the formation of landfast ice. Further simulations including thermodynamic effects are needed, however, to examine those scenarios of landfast ice formation. The results also predict the distributions of stresses, ice thickness, area coverage, and ridging. As may be expected, most of the ridging, and high stresses, occur near the land boundaries. Stresses along a land boundary were found to increase from the stress-free upstream inlet to reach a maximum, then decrease towards the downstream exit.

The present computations were also able to simulate the formation of an arch at the constricted exit of the channel. If the shear strength of the ice cover is sufficiently large, an arch was found to form. It was shown that the threshold shear strength needed to form an arch depends on the environmental driving force (wind speed in the present case) and the width of the channel. Note that the shear strength may be introduced by choosing a particular ratio of the major to minor axes for the elliptical yield envelope. One test case showed that ice may initially flow through the channel. Then, as the ice cover compresses (area coverage increases), the strength of the ice cover increases and eventually an arch forms and the flow comes to a stop.

A cursory comparison was done with the previous numerical simulations of Gutfraind and Savage (1998). Comparisons with field observations are undeway for verification of model prediction. Future work should also include an examination of thermodynamic effects on arch formation.

ACKNOWLEDGEMENTS

The support of the Panel on Energy Research and Development (PERD) is gratefully acknowledged.

REFERENCES

Brackbill, JU, Kothe, DB, and Ruppel, HM (1988). "FLIP: a low dissipation, particle-in-cell method for fluid flow*," Comput Phys Comm*, Vol 48, pp 25-38.

Erlingsson, B (1991). "The propagation of characteristics in sea-ice deformation fields," *Annals Glaciol,* Vol 15, pp 73-80.

Gutfraind, R, and Savage, S (1998). "Flow of fractured ice through wedge-shaped channels: smoothed particle hydrodynamics and discrete-element simulations," *Mech of Materials*, Vol 29, pp 1-17.

Harlow, FH (1964). "The Particle in Cell Computing Method for Fluid Dynamics," *Methods for Computational Physics*, Vol 3, pp 319-343.

Hibler III, WD (1979). "A dynamic thermodynamic sea ice model," *J Phys Ocean*, Vol 9, No 4, pp 815-846.

Hopkins, MA (1998). "Four stages of pressure ridging," *J Geophys Res*, Vol 103 (C10), pp 21883- 21891.

Jenike, AW (1964). "Steady gravityflow of frictional-cohesive solids in converging channels," *J Applied Mechanics,* Vol31, pp 5-11.

Kubat, I, Sayed, M, Carrieres, T, and Savage, S (2004). "Performance of the New Canadian Ice Service Ice Thickness Redistribution Model," *Proc Int Offshore and Polar Eng Conf*, ISOPE, Toulon, France, May 23-28, pp 855-862.

Kubat, I, Sayed, M, Savage, S, and Carrieres, T (2005). "Implementation and testing of a thickness redistribution model for operational ice forecasting," *Proc Int Conf on Port and Ocean Eng under Arctic Conditions,* POAC, Potsdam, NY, USA, June 26-30, Vol 2, pp 781-791.

Kwok, R, and Rothrock, DA (1999). "Variability of Fram Strait ice flux and North Atlantic oscillation," *J Geophys Res* , No 104, pp 5177-5189.

Kwok, R (2005). "Nares Strait ice flux," *Geophysical Research Letters*, Vol 32, L24502, doi:10.1029/2005GL024768.

Samelson, RM, Agnew, T, Melling, H, and Munchov, A (2005). "Evidence for atmospheric control of sea-ice motion through Nares Strait," *Geophysical Research Letters* , Vol 33, LXXX ,doi:10.1029/2005GL025016.

Savage, SB (2002). "Two category sea-ice thickness redistribution model," *Report prepared for Canadian Ice Service, Environment Canada, 373 Sussex Dr, Ottawa, Ontario, Canada, K1A 0H3, March 31, 2002.*

Sayed, M, and Carrieres, T (1999). "Overview of a new operational ice forecasting model," *Proc Int Offshore and Polar Eng Conf*, ISOPE, Brest, France, May 30- June 4, Vol II, pp 622-627.

Sayed, M, Carrieres, T, Tran, H and Savage, SB (2002). "Development of an operational ice dynamics model for the Canadian Ice Service," *Proc Int Offshore and Polar Eng Conf*, ISOPE, Kitakyushu, Japan , May 26-31, pp 841-848.

Sodhi, DS (1977). "Ice arching and the drift of pack ice through restricted channels," *CRREL Report 77-18, Hanover, New Hampshire, August 1977.*

Sulsky, D, and Brackbill, JU (1991). "A numerical method for suspension flow," *J Comput Phys,* Vol 96, pp 339-368.

Sulsky, D, Chen, Z, and Schryer, HL (1994). "Particle method for history-dependent materials," *Comput Methods Appl Mech Eng*, Vol 118, pp 179-196.

Zhang, J and Hibler III, WD (1997). "On an efficient numerical method for modelling sea ice dynamics," *J Geophysical Research*, Vol 102, No C4, pp 8691-8702.